

A numerical method for treating time-periodic boundary layers

By P. W. DUCK

Department of Mathematics, University of Manchester, Manchester M13 9PL, UK

(Received 11 March 1988 and in revised form 3 February 1989)

The development of an incompressible, laminar, pulsatile boundary layer over a semi-infinite flat plate is studied. Although the undisturbed free stream flow is taken to be non-reversing (following previous studies), sufficiently far downstream, the flow in part of the boundary layer must ultimately reverse direction during part of the cycle.

A novel numerical (finite-difference) scheme is described, which builds in the time periodicity of the flow, and also takes into account the direction of the flow in deciding the form of the differencing in the streamwise direction. The effect of variations in numerical grid is investigated, and comparison is made with asymptotic formulae applicable close to and far from the leading edge of the plate, together with linearized (small oscillation) results obtained using the analysis of Ackerberg & Phillips (1972), which is shown to yield remarkably accurate results when compared with the solution for the full problem, even for quite large oscillation amplitudes.

1. Introduction and formulation

In this paper the development of an incompressible, pulsatile boundary layer over a semi-infinite flat plate is discussed. The undisturbed free stream flow is taken to be $U_\infty(1 + \lambda \cos \omega t^*)$, parallel to the plate, with $|\lambda| < 1$ and so the free stream does not reverse direction. Within the framework of the classical boundary-layer formulation, the following problem results (see for example Pedley 1972):

$$\psi_{y,t^*} + \psi_y \psi_{xy} - \psi_x \psi_{yy} = -\lambda \omega U_\infty \sin \omega t^* + \nu \psi_{yyy}. \quad (1.1)$$

Here ψ is a dimensional stream function, and the velocity vector is then $(\psi_y, -\psi_x)$ referred to the Cartesian coordinates (x, y) . The boundary conditions (corresponding to zero fluid velocity on the surface $y = 0$, and matching with the free stream velocity) are

$$\left. \begin{aligned} \psi = \psi_y = 0 \quad \text{on} \quad y = 0, \quad x > 0, \\ \psi_y \rightarrow U_\infty(1 + \lambda \cos \omega t^*) \quad \text{as} \quad y \rightarrow \infty \end{aligned} \right\} \quad (1.2)$$

(together with free-stream conditions at $x = 0$).

The problem for $\lambda \ll 1$ has received a good deal of attention over the years. Some of the first investigations include those of Lighthill (1954), Lam & Rott (1960) and Ackerberg & Phillips (1972). Close to the leading edge of the plate the flow is basically Blasius in form, whilst downstream the solution takes on a double structure comprising an inner Stokes-type layer, together with an outer, Blasius-type layer. Numerical solutions extending from the leading edge of the plate to far downstream have been obtained for this linearized case ($\lambda \ll 1$) by Ackerberg & Phillips (1972) and by Goldstein, Pockol & Sanz (1983). The far downstream behaviour in this case

has been the subject of much discussion. In this limit (it is argued) a set of eigensolutions which decay exponentially fast in the streamwise direction must be present. One set of eigensolutions has been found by Lam & Rott (1960) and by Ackerberg & Phillips (1972); these are determined by conditions at the wall, and are characterized by a decay rate that decreases as the eigenvalue increases. A second set of eigenvalues has been found by Brown & Stewartson (1973*a, b*); these are determined by conditions on the outer edge of the boundary layer, and are characterized by a decay rate that increases with increasing order.

The problem for $\lambda = O(1)$, (but $|\lambda| < 1$) has also received some attention in the past. The asymptotic limit of close to the leading edge was studied by Moore (1951), (1957), and Pedley (1972), and the flow is found to be Blasius-like. The flow far from the leading edge which has been discussed by Lin (1956), Gibson (1957) and Pedley (1972), takes on a double structure, similar to that for $|\lambda| \ll 1$.

In this paper, the aim is to consider the solution to the $\lambda = O(1)$ problem, from the leading edge to far downstream, using a novel numerical method which incorporates the time-periodicity into the solution.

Non-dimensional and similarity-type variables t, η, ϕ , are introduced by

$$t^* = \frac{t}{\omega}, \quad y = \left[\frac{\nu x}{U_\infty} \right]^{\frac{1}{2}} \eta, \quad \psi = [\nu x U_\infty]^{\frac{1}{2}} \phi(\xi, \eta, t), \quad x = \frac{U_\infty}{\omega} \xi^2. \quad (1.3)$$

Before substitution into (1.1), a scaled streamwise variable is introduced (for numerical expediency), of the form

$$\xi = f(\bar{\xi}). \quad (1.4)$$

All the computations to be shown were obtained with

$$f(\bar{\xi}) = \tan^{-1} \bar{\xi}, \quad (1.5)$$

which results in a concentration of grid points close to the leading edge of the plate, $\xi = 0$, once discretization has been performed.

Equation (1.1) becomes

$$\phi_{\eta\eta\eta} + \frac{1}{2} \phi_{\eta\eta} \phi + \frac{1}{2} \bar{\xi} f'(\bar{\xi}) \phi_{\eta\eta} \phi_\xi - \frac{1}{2} f'(\bar{\xi}) \bar{\xi} \phi_\eta \phi_{\eta\xi} - \xi^2 \phi_{\eta t} = \bar{\xi}^2 \lambda \sin t. \quad (1.6)$$

Lin's (1956), Pedley's (1972) and related studies were restricted to cases for $|\lambda| < 1$, and asymptotic solutions in two limits, equivalent to $\bar{\xi} \ll 1$ and $\bar{\xi} \gg 1$ were considered. In particular flow reversal was shown to occur quite regularly in this problem.

At the leading edge of the plate, $\xi = 0$, (1.6) reduces to

$$\phi_{\eta\eta\eta} + \frac{1}{2} \phi_{\eta\eta} \phi = 0, \quad (1.7)$$

with boundary conditions

$$\left. \begin{aligned} \phi(\eta = 0) = \phi_\eta(\eta = 0) = 0, \\ \phi_\eta \rightarrow 1 + \lambda \cos t \quad \text{as } \eta \rightarrow \infty, \end{aligned} \right\} \quad (1.8)$$

which is a quasi-steady form of the Blasius problem (see for example Rosenhead 1963).

The conditions as $\bar{\xi} \rightarrow \infty$ are obtained from the work of Lin (1956) and Pedley (1972). Taking the leading-order terms as $\bar{\xi} \rightarrow \infty$ reveals the solution splitting into two components, namely

$$\phi \sim \phi_B(\eta) + \frac{\lambda}{\bar{\xi}} \phi_S(\eta \bar{\xi}, t), \quad (1.9)$$

where ϕ_B is the steady Blasius function (1.7)–(1.8) with $\lambda = 0$), and ϕ_S is the Stokes solution, namely

$$\phi_S(\hat{\eta}, t) = \frac{1}{2} \left\{ \hat{\eta} - \frac{(1-i)}{\sqrt{2}} [1 - e^{-(1+i)\hat{\eta}/\sqrt{2}}] \right\} e^{it} + \text{c.c.} \tag{1.10}$$

Equation (1.9) serves as a downstream boundary condition. Eigensolutions may occur, but are exponentially small as $\bar{\xi} \rightarrow \infty$ (although difficulties may occur much further downstream as described by Goldstein 1983).

Equation (1.9) describes a flow that (however small λ) must ultimately reverse for sufficiently large $\bar{\xi}$ during part of the time cycle (specifically when $\bar{\xi} = O(\lambda^{-1})$ as $\lambda \rightarrow 0$). As a result, any numerical scheme used to approximate (1.6) must be capable of correctly taking into account changes in flow direction.

2. Numerical method

One possible approach to this problem would be a time-marching procedure; however a number of difficulties could arise with such a scheme. First, the start-up process could provoke a singularity, such as arises in the problem of flow past a flat plate which is instantaneously moved from rest (see for example Hall 1969; Dennis 1972) or such as occurs in the flow on the surface of an impulsively translated circular cylinder (see for example van Dommelen & Shen 1980). Secondly, instabilities of the type described by Cowley, Hocking & Tutty (1985) of viscous form, associated with critical layers at points of zero shear, may be present and could cause numerical difficulties.

Instead, the approach here will be to build in the time periodicity of the solution, which eliminates any transient effects, by writing

$$\phi(\xi, \eta, t) = \sum_{n=-\infty}^{\infty} \phi_n(\xi, \eta) e^{int}, \tag{2.1}$$

and so
$$\phi_{-n}(\xi, \eta) = \text{complex conjugate } \{ \phi_n(\xi, \eta) \}, \tag{2.2}$$

in order that $\phi(\xi, \eta, t)$ is a real function. As a consequence of this it is necessary to consider only $n \geq 0$ in (2.1).

Substitution of (2.1) into (1.6) yields the following infinite set of equations:

$$\phi_{n\eta\eta} + \frac{1}{2} \sum_{j=-\infty}^{\infty} \phi_{n-j} \phi_{j\eta\eta} + \frac{1}{2} \bar{\xi} f'(\bar{\xi}) \{ \phi_{\eta\eta} \phi_{\xi} - \phi_{\eta} \phi_{\eta\xi} \}^n - in\xi^{-2} \phi_{n\eta} = \frac{1}{2} \xi^{-2} \lambda \delta_{1,|n|}, \tag{2.3}$$

where $\delta_{i,j}$ is the Kronecker delta, and $\{ \ }^n$ denotes the e^{int} component of the term inside the parenthesis.

The boundary conditions to be applied are

$$\left. \begin{aligned} \phi_n(\eta = 0) &= \phi_{n\eta}(\eta = 0) = 0, \\ \phi_{n\eta} &\rightarrow \delta_{n,0} + \frac{1}{2} \lambda \delta_{1,|n|} \quad \text{as } \eta \rightarrow \infty. \end{aligned} \right\} \tag{2.4}$$

A similar treatment for time periodic flows was used by Duck (1981, 1984), but these two studies both assumed non-reversing flow. The remaining question is the treatment of the ξ -derivatives in (2.3). At stations where the flow is forward at all times, there is no difficulty (see Duck 1981, 1984). However, at stations where the flow does change direction at certain times throughout the cycle, an appropriate numerical differencing scheme is required take this properly into account.

The key to the correct treatment may be obtained by considering a possible time-

marching approach to the problem. In this case if, at any (ξ, η) -station, at any time $\phi_\eta > 0$, the correct differencing in ξ would involve points from $\xi, \xi - \Delta\xi$ (and possibly $\xi - 2\Delta\xi, \xi - 3\Delta\xi$ etc. depending on the particular differencing scheme used), where $\Delta\xi$ denotes the grid spacing in ξ . This operation of differencing during forward-flow periods is written symbolically as D^+ . On the other hand, if the flow changes direction, and $\phi_\eta < 0$, then to ensure the correct zone of dependence (and hence numerical stability), the correct differencing scheme in ξ would involve points from $\xi, \xi + \Delta\xi$ (and possibly $\xi + 2\Delta\xi, \xi + 3\Delta\xi$, etc. again depending on the particular differencing scheme used). This operation of differencing during reversed-flow periods is written symbolically as D^- (and merely denotes upwind differencing).

A scheme is required to approximate $\phi_{\eta\xi}$ in (2.3), (ϕ_ξ will be treated similarly, although here this is not essential) if the flow reverses direction during the cycle. this turns out to be quite straightforward. The problem may be simply stated as follows; suppose that for $0 < t < t_0, \phi_\eta > 0$; for $t_0 < t < t_1, \phi_\eta < 0$; for $t_1 < t < 2\pi, \phi_\eta > 0$. The following difference approximations are then required:

$$\phi_{\eta\xi} \approx \begin{cases} D^+\phi_\eta & \text{for } \begin{cases} 0 < t < t_0 \\ t_1 \leq t < 2\pi \end{cases} \\ D^-\phi_\eta & \text{for } t_0 < t < t_1, \end{cases} \quad (2.5)$$

and so the n th component of the operation of differencing $\phi_{\eta\xi}$ in the ξ -direction may be obtained by evaluating the Fourier time series of (2.5). We have

$$\{\phi_{\eta\xi}\}^n \approx \sum_{\substack{m=-\infty \\ m \neq n}}^{\infty} \left\{ \frac{[e^{imt_0 - in t_0} - e^{imt_1 - in t_1}]}{2\pi(im - in)} (D^+ - D^-) \phi_{m\eta} \right\} + \frac{1}{2\pi} \{ (2\pi + t_0 - t_1) D^+ + (t_1 - t_0) D^- \} \phi_{n\eta}. \quad (2.6)$$

In situations for which: $0 < t < t_0, \phi_\eta < 0$; whilst for $t_0 < t < t_1, \phi_\eta > 0$; and for $t_1 < t < 2\pi, \phi_\eta < 0$, then it is necessary to interchange D^+ and D^- in (2.6). The scheme may also be extended to cases in which the flow changes direction on more than two occasions during the cycle.

Suppose the approximation to $\phi_{\eta\xi}$ is written as $D\phi_\eta$, then this operation may be written symbolically as

$$D\phi_\eta = \sum_{n=-\infty}^{\infty} \sum_{m=-\infty}^{\infty} (\mu_{n,m} D^+ \phi_{m\eta} + \nu_{n,m} D^- \phi_{m\eta}) e^{in t}. \quad (2.7)$$

Equation (2.3) may then be written as

$$\phi_{n\eta\eta} + \frac{1}{2} \sum_{j=-\infty}^{\infty} \phi_{n-j} \phi_{j\eta\eta} + \frac{1}{2} \xi \left\{ \sum_{j=-\infty}^{\infty} \left[\phi_{n-j\eta\eta} \sum_{m=-\infty}^{\infty} (\mu_{j,m} D^+ + \nu_{j,m} D^-) \phi_m - \phi_{n-j\eta} \sum_{m=-\infty}^{\infty} (\mu_{j,m} D^+ + \nu_{j,m} D^-) \phi_{m\eta} \right] \right\} - in \xi^{-2} \phi_{n\eta} = \frac{1}{2} \xi^{-2} \lambda \delta_{1, |n|}. \quad (2.8)$$

Second-order central-differencing in η (grid size $\Delta\eta$ with $0 \leq \eta \leq \eta_\infty$) and first-order differencing in ξ for both $\phi_\eta < 0$ and $\phi_\eta > 0$, (grid size $\Delta\xi$ with $0 \leq \xi \leq \xi_\infty$) were used. For example

$$\phi_{n\eta\eta} \approx [\phi_n(\xi, \eta + 2\Delta\eta) - 3\phi_n(\xi, \eta + \Delta\eta) + 3\phi_n(\xi, \eta) - \phi_n(\xi, \eta - \Delta\eta)] / (\Delta\eta)^3, \quad (2.9)$$

$$D^+ \phi_n \approx [\phi_n(\xi, \eta + \Delta\xi) + \phi_n(\xi, \eta) - \phi_n(\xi - \Delta\xi, \eta + \Delta\xi) - \phi_n(\xi - \Delta\xi, \eta)] / 2\Delta\xi, \quad (2.10)$$

$$D^- \phi_n(\xi, \eta) \approx [\phi_n(\xi + \Delta\xi, \eta + \Delta\xi) + \phi_n(\xi + \Delta\xi, \eta) - \phi_n(\xi, \eta + \Delta\xi) - \phi_n(\xi, \eta)] / 2\Delta\xi. \quad (2.11)$$

The series (2.1) was truncated at $n = \pm N$, and the following (dual iteration) procedure was employed.

The difference approximation to (1.7) and (1.8) was solved (iteratively) with $\phi(\xi = 0)$ expanded in the truncated form of (2.1) (this amounts to solving the discretized approximation to (2.3) and (2.4) with $\xi = 0$). In the case of the $n = 0$ mode, a form of Newton's method was used (Gaussian elimination being used to solve the quadradiagonal system), whilst all other ϕ_n were solved for directly. All modes were considered sequentially, until convergence was deemed to have been achieved (usually based on the maximum change of any of the $|\phi_0(\eta)|$). Some appropriate 'guess' was then made for all other modes, at all other ξ -values (with (1.9) and (1.10) imposed at the extreme downstream location, $\xi = \xi_\infty$).

The computation then proceeded to the next ξ -station ($\xi = \Delta\xi$). Here an iteration similar to that employed at $\xi = 0$ was used. However, at each point ($\xi > 0, \eta + \frac{1}{2}\Delta\eta$), at a given iteration, it is necessary to consider:

- (i) if the flow changes direction (determined by whether

$$\begin{aligned} \phi_\eta(\xi, \eta + \frac{1}{2}\Delta\eta, t) &= \sum_{n=-N}^N \phi_{n\eta}(\xi, \eta + \frac{1}{2}\Delta\eta) e^{int} \\ &\approx \sum_{n=-N}^N \frac{\phi_n(\xi, \eta + \Delta\eta) - \phi_n(\xi, \eta)}{\Delta\eta} e^{int} \end{aligned} \tag{2.12}$$

changes sign during $0 \leq t \leq 2\pi$;

- (ii) the direction of the flow at $t = 0$ (obtained by evaluating (2.12) at $t = 0$);

(iii) if the answer to (i) is affirmative, then the times of flow reversal (t_0, t_1) are determined, by means of evaluating the zeros of (2.12).

NAG routines CO5ADF, CO5AXF (which evaluate the zeros of a continuous function) and EO4BBF (which finds the minimum of a continuous function) were used to answer questions (i) and (iii).

The various modes were solved sequentially, in the manner described above, until convergence was achieved. Note that if the flow does not change direction at any time throughout the cycle, for $0 < \xi < \xi_c$, then the ϕ_n over this range are then completely determined.

Once the solution up to $\xi = \xi_\infty - \Delta\xi$ was attained in the manner described above, a second (outer) iteration was imposed, the calculation for stations lying in the range $\xi_c \leq \xi \leq \xi_\infty$ being considered yet again, repeating the procedure described above, in order that information is correctly propagated upstream (relative to the free-stream flow). Convergence of this outer iteration was generally considered to have been satisfied when the maximum change in any of the modes of the wall shear at any of the ξ between ξ_c and ξ_∞ , fell below some suitably small value. The computation was then considered to be converged.

3. Results

The example $\lambda = 0.5$ was chosen to test the method. In all the computations shown here, (1.5), was used over the range $0 < \xi < \frac{1}{2}\pi - 0.1$ (i.e. $\xi_\infty = \frac{1}{2}\pi - 0.1$), giving $0 < \bar{\xi} < 9.967$. This example was computed on grids A-I, as described in table 1.

Figure 1 shows the results for $\phi_{0\eta\eta}(\eta = 0)$ -distributions with x (the $n = 0$ mode is of course real), together with the corresponding $\text{Im}\{\phi_{1\eta\eta}(\eta = 0)\}$ -distributions, as obtained from the various computations A-I. These values of $\phi_{n\eta\eta}$ were obtained from the (converged) results for ϕ_n , by means of the approximation

$$\phi_{nm}(\xi, 0) \approx [-5\phi_n(\xi, \Delta\eta) + 4\phi_n(\xi, 2\Delta\eta) - \phi_n(\xi, 3\Delta\eta)]/(\Delta\eta)^2, \tag{3.1}$$

Computation	N	λ	$\Delta\xi$	η_∞	$\Delta\eta$
A	4	0.5	0.03676	5	0.03125
B	4	0.5	0.03676	5	0.125
C	4	0.5	0.03676	5	0.0625
D	4	0.5	0.03676	10	0.125
E	4	0.5	0.07354	5	0.125
F	2	0.5	0.07354	5	0.125
G	9	0.5	0.03676	5	0.125
H	4	0.5	0.03676	10	0.625
I	4	0.5	0.04903	5	0.125
J	4	0.75	0.03676	10	0.0625

TABLE 1. Computation parameters

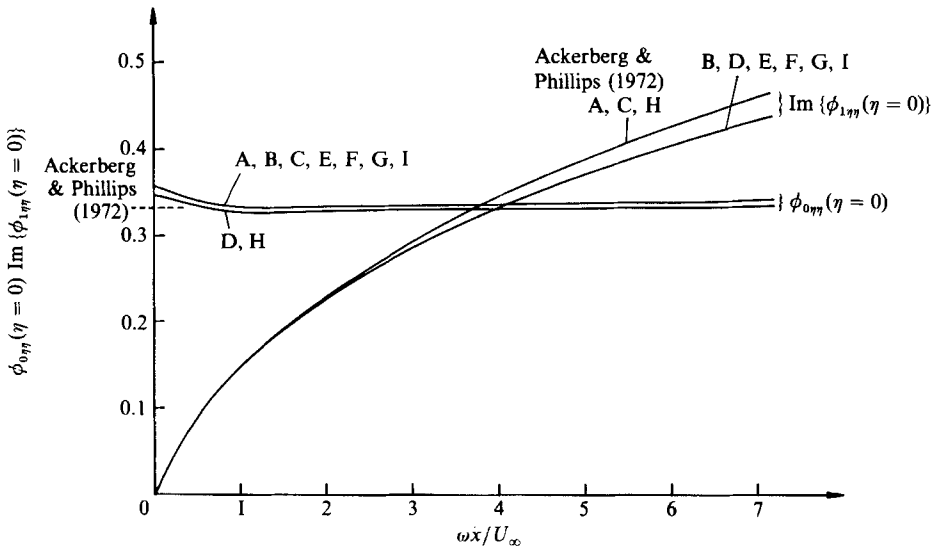


FIGURE 1. Distribution of $\text{Im}(\phi_{1,\eta}|_{\eta=0})$ and $\phi_{0,\eta}|_{\eta=0}$; $\lambda = \frac{1}{2}$.

an approximation that was found to be considerably more accurate than the more compact, but less accurate, first-order approximation originally used by the author. The $n = 0$ mode seems quite insensitive to changes in any of the grid sizes, but does seem a little dependent on η_∞ , even close to $x = 0$. On the other hand $\text{Im}(\phi_{n,\eta}(\eta =))$ is quite insensitive to η_∞ (and also to $\Delta\xi$), but is rather more sensitive to $\Delta\eta$, particularly for the larger values of x . The reason for this can be seen quite clearly by referring to the downstream condition (1.9). As $\bar{\xi} \rightarrow \infty$, the unsteady boundary layer is becoming progressively thinner relative to the η -scale (as $\bar{\xi}^{-1}$), although in terms of the unscaled y -coordinate the Stokes layer thickness becomes independent of x , and it is the steady boundary-layer thickness that grows on this scale. Hence as $\bar{\xi}$ becomes larger, a progressively smaller $\Delta\eta$ is required in order to describe adequately the unsteady component of the solution.

The linearized analysis of Ackerberg & Phillips (1972) assumes a constant value of $\phi_{0,\eta}|_{\eta=0}$ (equal to the Blasius value), and this is shown as a broken line on the vertical scale. The largest deviation of the present nonlinear results is clearly seen to occur at $x = 0$, whilst in the limit $x \rightarrow \infty$, $\phi_{0,\eta}|_{\eta=0}$ of course approaches this value.

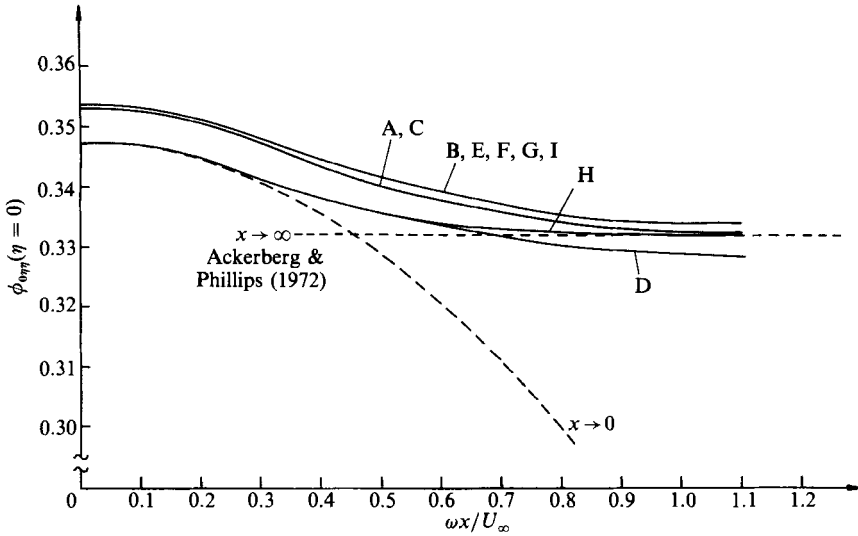


FIGURE 2. Comparison of computed distributions of $\phi_{0\eta\eta}|_{\eta=0}$ for $\lambda = \frac{1}{2}$, with $\bar{\xi} \ll 1$ and $\bar{\xi} \gg 1$ asymptotic solutions.

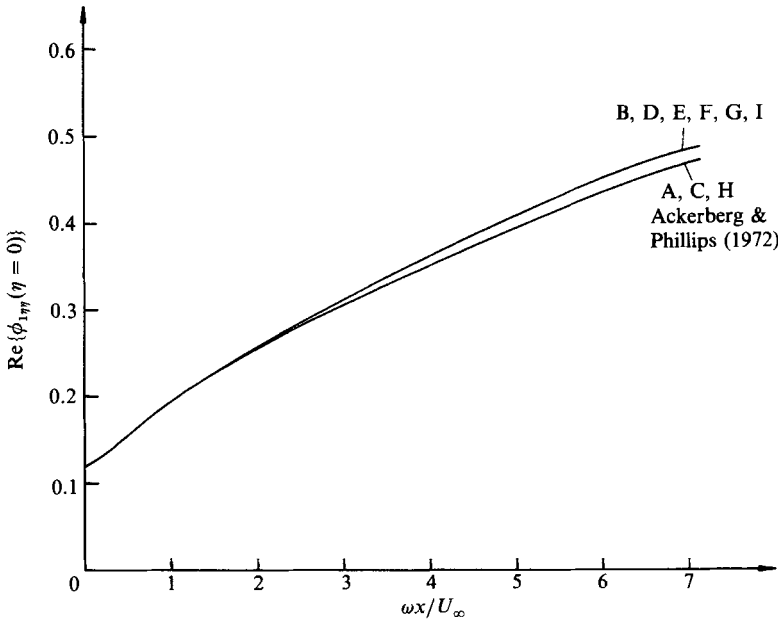


FIGURE 3. Distribution of $\text{Re}\{\phi_{1\eta\eta}|_{\eta=0}\}$; $\lambda = \frac{1}{2}$.

The linearized results of Ackerberg & Phillips (1972) were recomputed, using a greatly simplified version of the computer code used for the fully non-linear problem (just one mode, $n = 1$, is computed, by a straightforward marching technique in ξ involving no iteration). The results for $\text{Im}\{\phi_{1\eta\eta}|_{\eta=0}\}$ with $\lambda = 0.5$ were found to be indistinguishable from our (most accurate) nonlinear results, on the scale used in figure 1.

It is interesting to gauge the usefulness of the asymptotic expansions, equivalent to $\bar{\xi} \ll 1$ and $\bar{\xi} \gg 1$ which have appeared in past literature. Figure 2 shows results (on

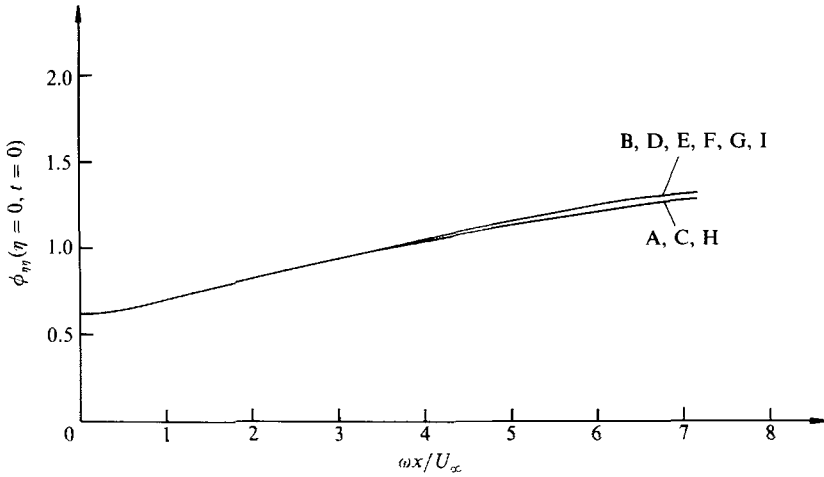


FIGURE 4. Distribution of $\phi_{\eta\eta}|_{\eta=0}$, $\lambda = \frac{1}{2}$ at $t = 0$.

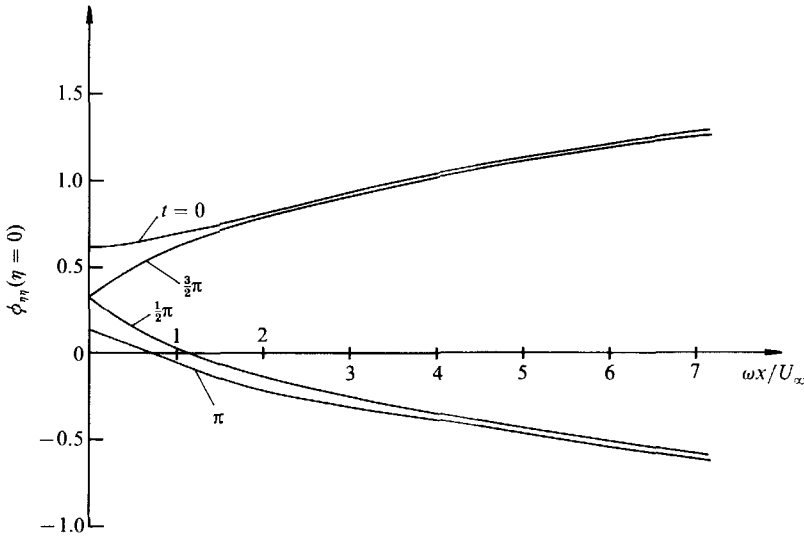


FIGURE 5. Distribution of $\phi_{\eta\eta}|_{\eta=0}$, $\lambda = \frac{1}{2}$ at times indicated.

an enlarged scale) for $\phi_{0\eta\eta}(\eta = 0)$ obtained from computations A-I. Also indicated, as broken lines, are the three-term expansion for $\bar{\xi} \ll 1$ (e.g. Pedley 1972), and the one-term expansion for $\bar{\xi} \gg 1$, i.e. the Blasius result which therefore corresponds to the Ackerberg & Phillips (1972) value (as noted by Pedley 1972, there is difficulty in obtaining further terms in this expansion, owing to the presence of eigensolutions). Figure 2 indicates that $\bar{\xi}^2 \doteq 0.47$ is the crossover point where the two expansions coincide (agreeing with the value found by Pedley 1972). Figure 3 shows the downstream distribution of $\text{Re}\{\phi_{1\eta\eta}(\eta = 0)\}$, and again the effects of changes in grid are shown. Our previous remarks concerning the effect of grid changes on $\text{Im}\{\phi_{1\eta\eta}(\eta = 0)\}$ are again applicable, as in the comment regarding the closeness of these results to those of Ackerberg & Phillips (1972).

In a further (final) attempt to assess the effect of grid changes, in figure 4 we show the distribution of $\phi_{\eta\eta}(\eta = 0, x, t = 0)$. Again, the primary source of numerical error

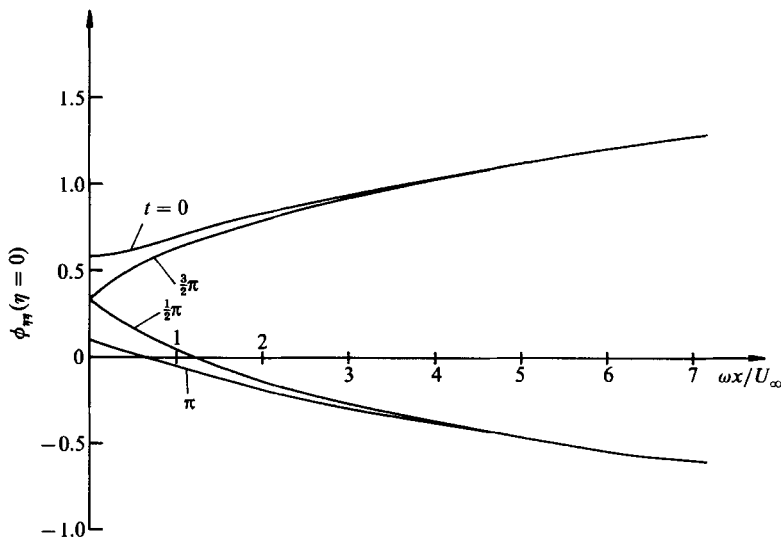


FIGURE 6. Distribution of $\phi_{\eta\eta}|_{\eta=0}$, $\lambda = \frac{1}{2}$ at times indicated (linearized results).

is seen to be the finiteness of $\Delta\eta$ (although the second-order accuracy of the scheme with $\Delta\eta$ is confirmed). It is particularly noteworthy here (confirmed by detailed inspection of the computed results), how insignificant changes in the number of Fourier modes (i.e. N) are. Indeed, the amplitudes of the higher modes (i.e. $|n| \geq 2$) were never more than 7% of the amplitude of the $|n| = 1$ mode (this maximum occurring at $x = 0$). The present problem appears not to be highly nonlinear (the primary effect of nonlinearity is to cause the small but perceptible derivation of ϕ_0 from the Blasius solution). However, it would appear likely that if the scheme were to be applied to a problem admitting fast temporal growths (such as in a problem involving the approach of a singularity), then significant numbers of Fourier terms could well be necessary.

Inspection of the results overall suggests that of all the grids employed, computation H gave the most accurate overall results, and the remainder of the results to be shown were computed with this grid.

Figure 5 shows distributions of $\phi_{\eta\eta}(\eta = 0, x, t)$ for $\lambda = 0.5$ with x , at four times during the cycle. This shows that flow reversal can occur quite close to the leading edge. For comparison, figure 6 shows the equivalent linear distributions obtained from the analysis of Ackerberg & Phillips (1972) (but computed with our modified code), with their small parameter ϵ (λ in our notation) set equal to 0.5. These results are seen to give a remarkably good description of the full problem.

Figures 7(a), 7(b) and 7(c) show instantaneous velocity profiles at $t = 0, \frac{1}{2}\pi, \pi, \frac{3}{2}\pi$ for $\omega x/U_\infty = 0, 1.7192$ and 3.9200 respectively (for the full problem). The development of reversed flow downstream is clearly observed, as is the downstream formation of a sub-(Stokes) layer.

We now turn our attention to a larger value of oscillation parameter, namely $\lambda = 0.75$. This case was evaluated using the grid described by computation J (whose grid was comparable with that of computation H).

Figure 8 shows the distribution of $\phi_{\eta\eta}(\eta = 0, x, t)$ with x at $t = 0, \frac{1}{2}\pi, \pi, \frac{3}{2}\pi$. These exhibit broadly the same characteristics as the corresponding $\lambda = 0.5$ results (figure 5), although we see that at $t = \pi$, the reversal point on the wall has moved

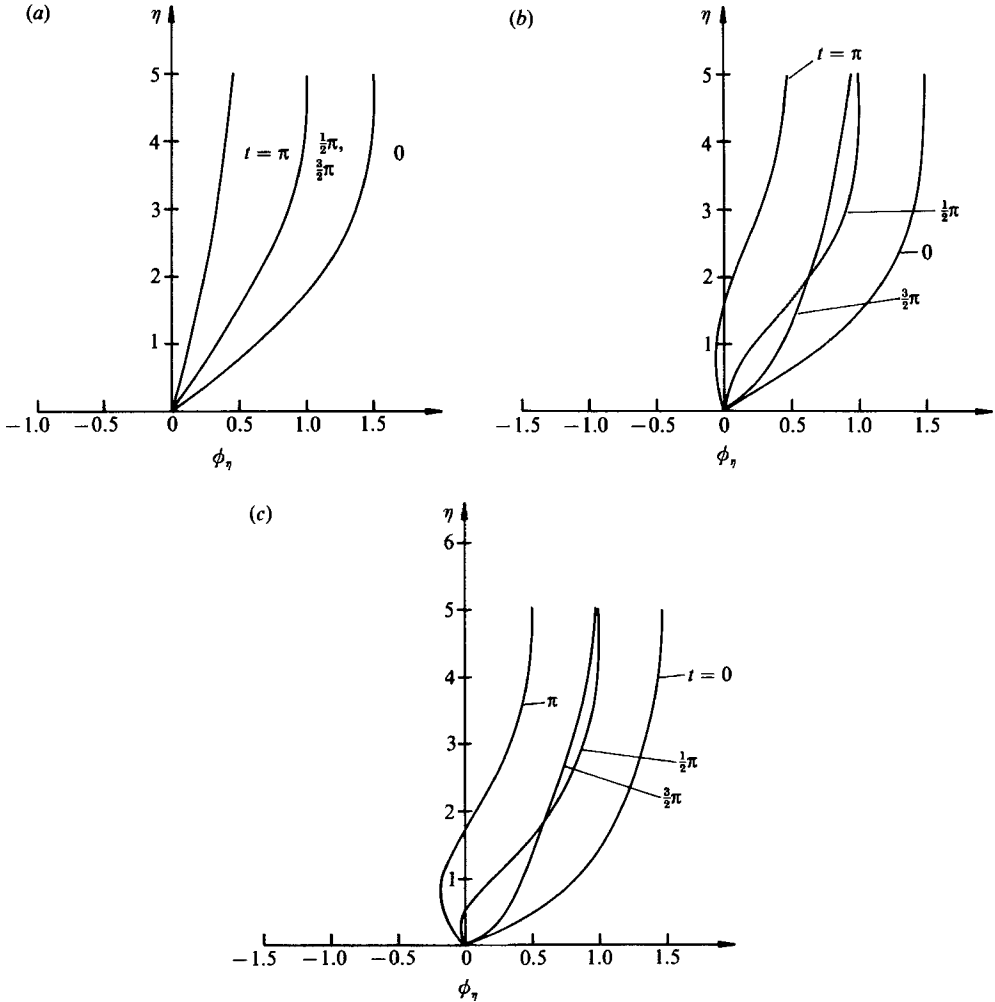


FIGURE 7. Instantaneous velocity profiles at $\lambda = \frac{1}{2}$: (a) $x = 0$; (b) $\omega x / U_\infty = 1.7192$; (c) $\omega x / U_\infty = 3.9200$.

considerably nearer the leading edge. The corresponding results obtained using the linearized Ackerberg & Phillips (1972) analysis, by setting $\lambda = 0.75$, are shown in figure 9. Although these give a generally good representation of the full solution, it is noteworthy that at $t = \pi$ it is predicted that $\phi_{0\eta}(\eta = 0, x, \pi) < 0$, in clear violation of our basic assumptions.

Figures 10(a), 10(b) and 10(c) show instantaneous velocity profiles (for the nonlinear problem) at $t = 0, \frac{1}{2}\pi, \pi, \frac{3}{2}\pi$ for $\omega x / U_\infty = 0, 1.7192$ and 3.9200 respectively. Here, the region of reversed flow is seen to be increased.

It is expected that $\lambda \geq 1$ are all singular cases, since then flow reversal would occur at/ahead of the leading edge during periods of the cycle.

In conclusion, the numerical method introduced here, involving a decomposition of the solution into a Fourier (time) series, together with what is believed to be a correct differencing scheme for reversing flows, seems to be efficient, although this particular problem does not appear to be highly nonlinear. The scheme is generally

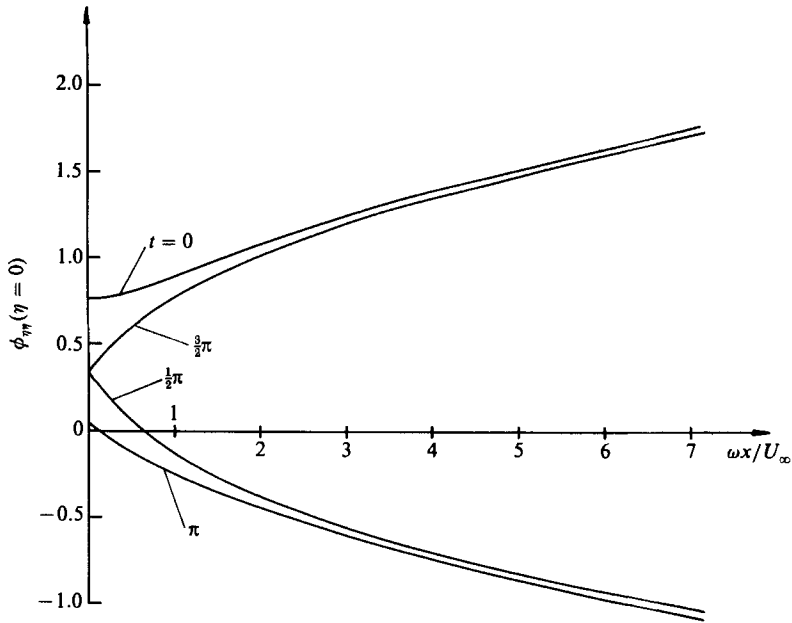


FIGURE 8. Distribution of $\phi_{\eta\eta}|_{\eta=0}$, $\lambda = \frac{3}{4}$ at times indicated.

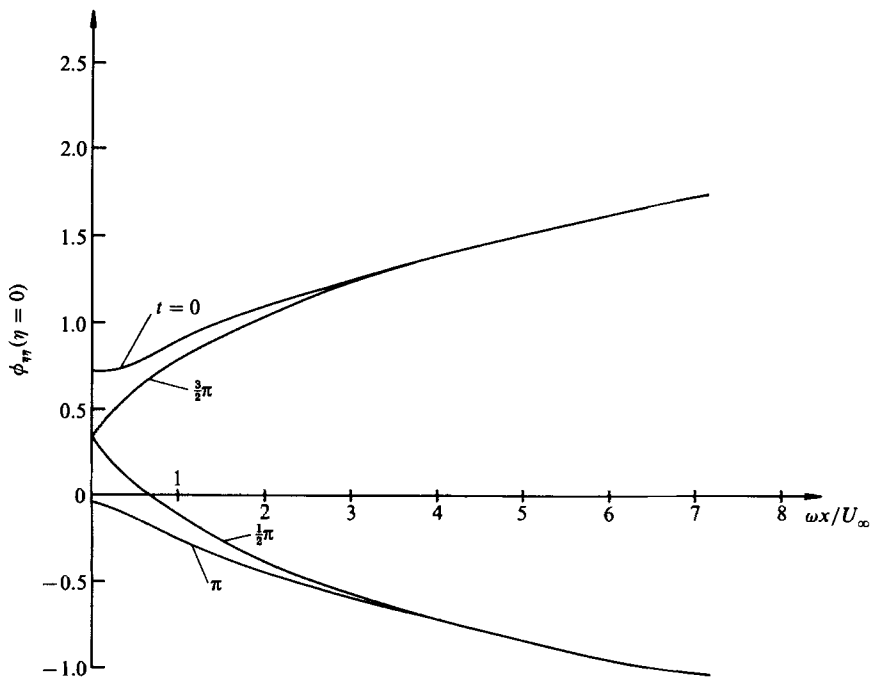


FIGURE 9. Distribution of $\phi_{\eta\eta}|_{\eta=0}$, $\lambda = \frac{3}{4}$ at times indicated (linearized results).

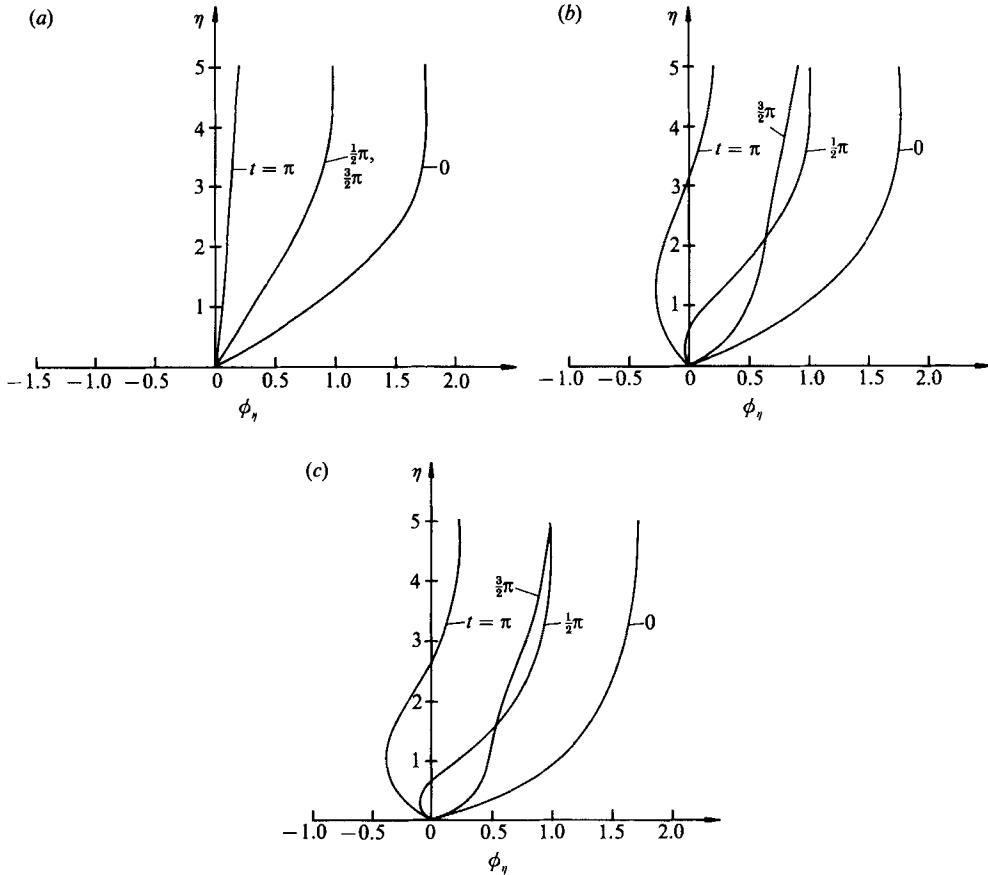


FIGURE 10. Instantaneous velocity profiles at $\lambda = \frac{3}{4}$: (a) $x = 0$; (b) $\omega x/U_\infty = 1.7192$;
(c) $\omega x/U_\infty = 3.9200$.

suitable for time-periodic boundary-layer flows which reverse regularly, and the author has obtained solutions to other examples using this approach, which compare favourably with corresponding time-marching solutions.

This work was partially supported by NATO Grant 523/82. A number of the computations were carried out at the University of Manchester Regional Computer Centre, with computer time provided under SERC Grant No. GR/E/25702.

REFERENCES

- ACKERBERG, R. L. & PHILLIPS, J. H. 1972 The unsteady boundary layer on a semi-infinite flat plate due to small fluctuations in the magnitude of the free-stream velocity. *J. Fluid Mech.* **51**, 137.
- BROWN, S. N. & STEWARTSON, K. 1973a On the propagation of disturbances in a laminar boundary layer I. *Proc. Camb. Phil. Soc.* **73**, 493.
- BROWN, S. N. & STEWARTSON, K. 1973b On the propagation of disturbances in a laminar boundary layer II. *Proc. Camb. Phil. Soc.* **73**, 503.
- COWLEY, S. J., HOCKING, L. M. & TUTTY, O. R. 1985 On the stability of solutions of the classical unsteady boundary-layer equations. *Phys. Fluids* **20**, 441.

- DENNIS, S. C. R. 1972 The motion of a viscous fluid past an impulsively started semi-infinite plate. *J. Inst. Maths Applics* **10**, 105.
- DOMMELEN, L. L. VAN & SHEN, S. F. 1980 The spontaneous generation of the singularity in a separating laminar boundary layer. *J. Comp. Phys.* **30**, 125.
- DUCK, P. W. 1981 Torsional oscillations of a finite disk. *SIAM J. Appl. Maths* **41**, 247.
- DUCK, P. W. 1984 The interaction between a steady laminar boundary layer and an oscillatory flap the condensed problem. In *Numerical and Physical Aspects of Aerodynamic Flows II* (ed. T. Cebeci). Springer.
- GIBSON, W. E. 1957 Unsteady boundary layers. Ph.D. dissertation, MIT.
- GOLDSTEIN, M. E. 1983 The evolution of Tollmien-Schlichting waves near a leading edge. *J. Fluid Mech.* **127**, 59.
- GOLDSTEIN, M. E., POCKOL, P. M. & SANZ, J. 1983 The evolution of Tollmien-Schlichting waves near a leading-edge. Part 2. Numerical determination of amplitudes. *J. Fluid Mech.* **129**, 443.
- HALL, M. G. 1969 The boundary layer on an impulsively started flat plate. *Proc. R. Soc. Lond. A* **320**, 332.
- LAM, S. H. & ROTT, N. 1960 Theory of linearised time-dependent boundary layers. *Cornell Univ. GSAE Rep.* AF0512 TN-60-1100.
- LIGHTHILL, M. J. 1954 The response laminar skin friction and heat transfer to fluctuations in the stream velocity. *Proc. R. Soc. Lond. A* **224**, 1.
- LIN, C. C. 1956 Motion in the boundary layer with a rapidly oscillatory external flow. *Proc. IX Intl Appl. Mech. Brussels*, vol. 4, p. 155.
- MOORE, F. K. 1951 Unsteady laminar boundary layer flow. *NACA Tech. Note* 2471.
- MOORE, F. K. 1957 Aerodynamic effects of boundary-layer unsteadiness. *Proc. 6th Anglo-Amer. Conf. R. Aero. Soc. Folkstone*, p. 439.
- PEDLEY, T. J. 1972 Two-dimensional boundary layers in a free stream which oscillates without reversing. *J. Fluid Mech.* **55**, 359.
- ROSENHEAD, L. (ed) 1963 *Laminar Boundary Layers*. Oxford University Press.